

AD-A080 117

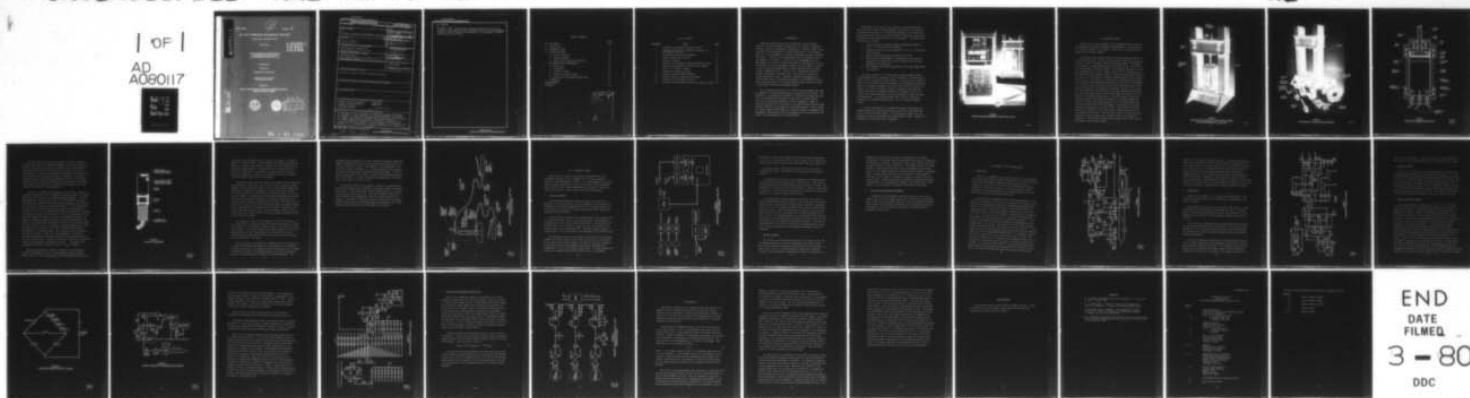
TEXAS UNIV AT AUSTIN APPLIED RESEARCH LABS  
THE ARL:UT SUBSEAFLOOR ENVIRONMENTAL SIMULATOR.(U)  
NOV 79 D J SHIRLEY  
UNCLASSIFIED ARL-TR-79-53

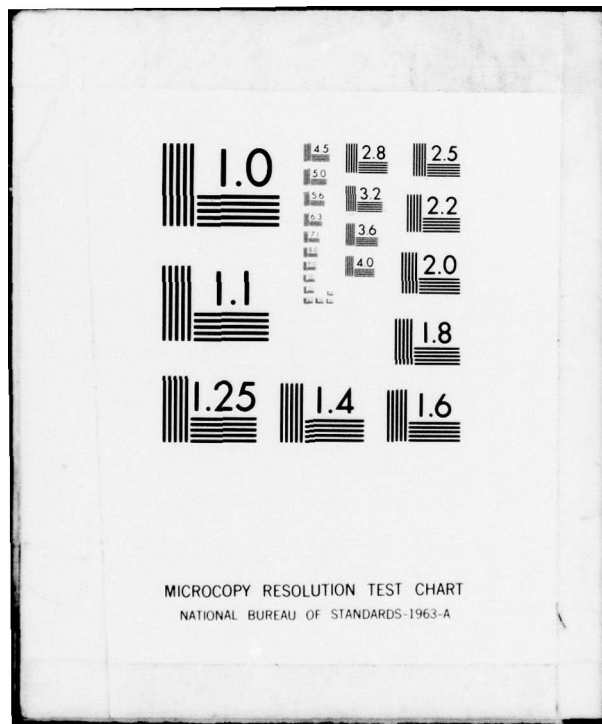
F/6 8/10

N00014-77-C-0779

NL

| OF |  
AD  
A080117





MICROCOPY RESOLUTION TEST CHART  
NATIONAL BUREAU OF STANDARDS-1963-A

ADA080117

ARL-TR-79-53

12  
P.S.

Copy No. 14

**THE ARL:UT SUBSEAFLOOR ENVIRONMENTAL SIMULATOR**

Final Report under Contract N00014-77-C-0779

Donald J. Shirley

LEVEL

**APPLIED RESEARCH LABORATORIES**  
THE UNIVERSITY OF TEXAS AT AUSTIN  
POST OFFICE BOX 9829, AUSTIN, TEXAS 78712

29 November 1979

Technical Report

1 September 1977 - 31 December 1979

APPROVED FOR PUBLIC RELEASE;  
DISTRIBUTION UNLIMITED.

Prepared for:

**NAVAL OCEAN RESEARCH AND DEVELOPMENT ACTIVITY**  
NSTL STATION, MS 39529

DDC FILE COPY



DDC  
RECEIVED  
FEB 1 1980  
A

80 1 31 003

UNCLASSIFIED

SECURITY CLASSIFICATION OF THIS PAGE (When Data Entered)

REPORT DOCUMENTATION PAGE		READ INSTRUCTIONS BEFORE COMPLETING FORM
1. REPORT NUMBER	2. GOVT ACCESSION NO.	3. RECIPIENT'S CATALOG NUMBER
4. TITLE (and Subtitle)		5. TYPE OF REPORT & PERIOD COVERED
6 THE ARL:UT SUBSEAFLOOR ENVIRONMENTAL SIMULATOR		final report 1 Sep 77 - 31 Dec 79
7. AUTHOR(s)		PERFORMING ORG. REPORT NUMBER
10 Donald J. / Shirley		14 ARL-TR-79-53
9. PERFORMING ORGANIZATION NAME AND ADDRESS		15. CONTRACT OR GRANT NUMBER(s)
Applied Research Laboratories The University of Texas at Austin Austin, Texas 78712		15 N00014-77-C-0779
11. CONTROLLING OFFICE NAME AND ADDRESS		10. PROGRAM ELEMENT, PROJECT, TASK AREA & WORK UNIT NUMBERS
Commanding Officer Naval Ocean Research and Development Activity NSTL Station, MS 39529		12 39
14. MONITORING AGENCY NAME & ADDRESS (if different from Controlling Office)		12. REPORT DATE
		11 29 November 1979
		13. NUMBER OF PAGES
		15. SECURITY CLASS. (of this report)
		UNCLASSIFIED
		15a. DECLASSIFICATION/DOWNGRADING SCHEDULE
		N/A
16. DISTRIBUTION STATEMENT (of this Report)		
Approved for public release; distribution unlimited.		
17. DISTRIBUTION STATEMENT (of the abstract entered in Block 20, if different from Report)		
18. SUPPLEMENTARY NOTES		
19. KEY WORDS (Continue on reverse side if necessary and identify by block number)		
sediment acoustical properties                      temperature sediment thermal properties                      simulation hydrostatic pressure overburden pressure		
20. ABSTRACT (Continue on reverse side if necessary and identify by block number)		
An instrument has been constructed to simulate the natural environment of the subseafloor so that acoustical and thermal measurements can be made on a sediment at temperatures and pressures that duplicate in the laboratory those found in the natural environment. Hydrostatic pressures to $5.2 \times 10^8$ dyn/cm <sup>2</sup> can be achieved by the instrument to simulate actual sediment pore pressure. Frame or overburden pressure can be exerted on the sediment up to $1.7 \times 10^8$ dyn/cm <sup>2</sup> . Specimen temperature can be regulated		

DD FORM 1473 1 JAN 73 EDITION OF 1 NOV 65 IS OBSOLETE

UNCLASSIFIED

SECURITY CLASSIFICATION OF THIS PAGE (When Data Entered)

TIMES 404 434

JOB

UNCLASSIFIED

SECURITY CLASSIFICATION OF THIS PAGE(When Data Entered)

20. (Cont'd)

from 0°C to 75°C. The instrument includes transducers and electronic equipment to make shear wave and compressional wave acoustic measurements as well as thermal conductivity measurements on the sediment at selected temperatures and pressures.

UNCLASSIFIED

SECURITY CLASSIFICATION OF THIS PAGE(When Data Entered)

TABLE OF CONTENTS

	<u>Page</u>
LIST OF FIGURES	v
I. INTRODUCTION	1
II. MECHANICAL SYSTEM	5
III. ELECTRONIC SYSTEM	15
A. Acoustic Subsystem	15
B. Thermal Subsystem	17
C. Pressure and Displacement Subsystem	18
IV. ELECTRONIC CIRCUIT DESCRIPTIONS	19
A. Power Pulser	19
B. Preamplifier	21
C. Thermistor Bridge	23
D. Thermal Conductivity Bridge	23
E. Pressure and Displacement Display Unit	28
V. CALIBRATION	31
ACKNOWLEDGMENTS	35
REFERENCES	37

Accession For	
NTIS GRA&I	<input checked="" type="checkbox"/>
DDC TAB	<input type="checkbox"/>
Unannounced	<input type="checkbox"/>
Justification	
By _____	
Distribution/	
Availability Codes	
Dist	Avail and/or special
A	

LIST OF FIGURES

<u>Figure No.</u>	<u>Title</u>	<u>Page</u>
1	Subseafloor Environmental Simulator System	3
2	Assembled Pressure Case and Hydraulic Press of the Environmental Simulator	6
3	Environmental Simulator Disassembled	7
4	Pressure Chamber Cross-Section	8
5	Acoustic Transducer	10
6	Subseafloor Environmental Simulator Hydraulic System	13
7	Subseafloor Environmental Simulator Block Diagram	16
8	Power Pulser Schematic Diagram	20
9	Preamplifier Schematic Diagram	22
10	Thermistor Bridge Schematic Diagram	24
11	Thermal Conductivity Bridge Block Diagram	25
12	Thermistor Bridge Schematic Diagram	27
13	Pressure and Displacement Display Unit Schematic Diagram	29

## I. INTRODUCTION

Acoustical properties and their relationship to other physical properties of ocean sediments are important to the fields of underwater acoustics, physical oceanography, and geophysics. Basically there are two approaches to the measurement of sediment properties: in situ measurements in a real environment and laboratory measurements using a simulated environment. Although in situ measurements have the advantage that the environment is the natural one, there are the disadvantages that the measurements are difficult to make, the degree of disturbance is not easy to determine, and the environmental parameters are not subject to control so that one must make measurements in widely separated areas to obtain a range of parameter values. Moreover, due to limitations imposed by available measurement techniques, the in situ method can yield only limited quantities of data. Conversely, laboratory measurements can easily be made using a controlled environment to vary parameters and can yield large quantities of useful data provided proper attention is given to measurement techniques and equipment design.

The two dominant properties of the ocean bottom environment that must be simulated in laboratory measurements are temperature and pressure. The temperature of unconsolidated sediments in the bottom can range from near 0°C at the sediment-water interface to near 100°C at greater depths. There are two pressures encountered in natural sediments: frame, or overburden pressure due to the weight of the mineral grains, and pore fluid pressure resulting from the weight of the overlying water. Thus to obtain an accurate simulated environment for laboratory studies of sediments, the temperature, frame pressure, and pore pressure must be controlled over the range of values encountered in the ocean bottom.

The purpose of this report is to describe an instrument which has been designed and built at Applied Research Laboratories, The University of Texas at Austin (ARL:UT), to enable the measurement of acoustical and other physical properties of real and artificial sediments at temperatures and pressures that simulate the real ocean environment. The system capabilities are as follows:

1. Achieve and hold a simulated sediment overburden pressure of 0 to  $1.7 \times 10^8$  dyn/cm<sup>2</sup> (0 to 2500 psi).
2. Achieve and hold a pore fluid pressure of 0 to  $5.2 \times 10^8$  dyn/cm<sup>2</sup> (0 to 7500 psi).
3. Maintain specimen temperature between 0° and 75°C.
4. Make acoustical measurements of compressional wave speed and attenuation and shear wave speed and attenuation at the above temperatures and pressures.
5. Make thermal conductivity measurements at the above temperatures and pressures.

The system consists of a stainless steel pressure chamber capable of withstanding the test pressures, with a hydraulically activated porous piston to exert the required frame pressure. An input port is included to allow the fluid pressure inside the chamber to be independently controlled. Acoustic and thermal transducers are rigidly mounted on the bottom of the chamber. The rest of the system consists of commercial and laboratory constructed electronic equipment mounted in an equipment rack for the acoustic and thermal measurements and the measurement of sample pressures and temperatures. A circulating thermal bath is used to control the temperature of the sample and container. Figure 1 shows the complete system.

In the following sections, the mechanical system consisting of the pressure chamber and associated hydraulic system will be described separately from the electronic system. In the electronic system, only the laboratory constructed equipment will be described in detail. Set-up and calibration of the system will be explained.

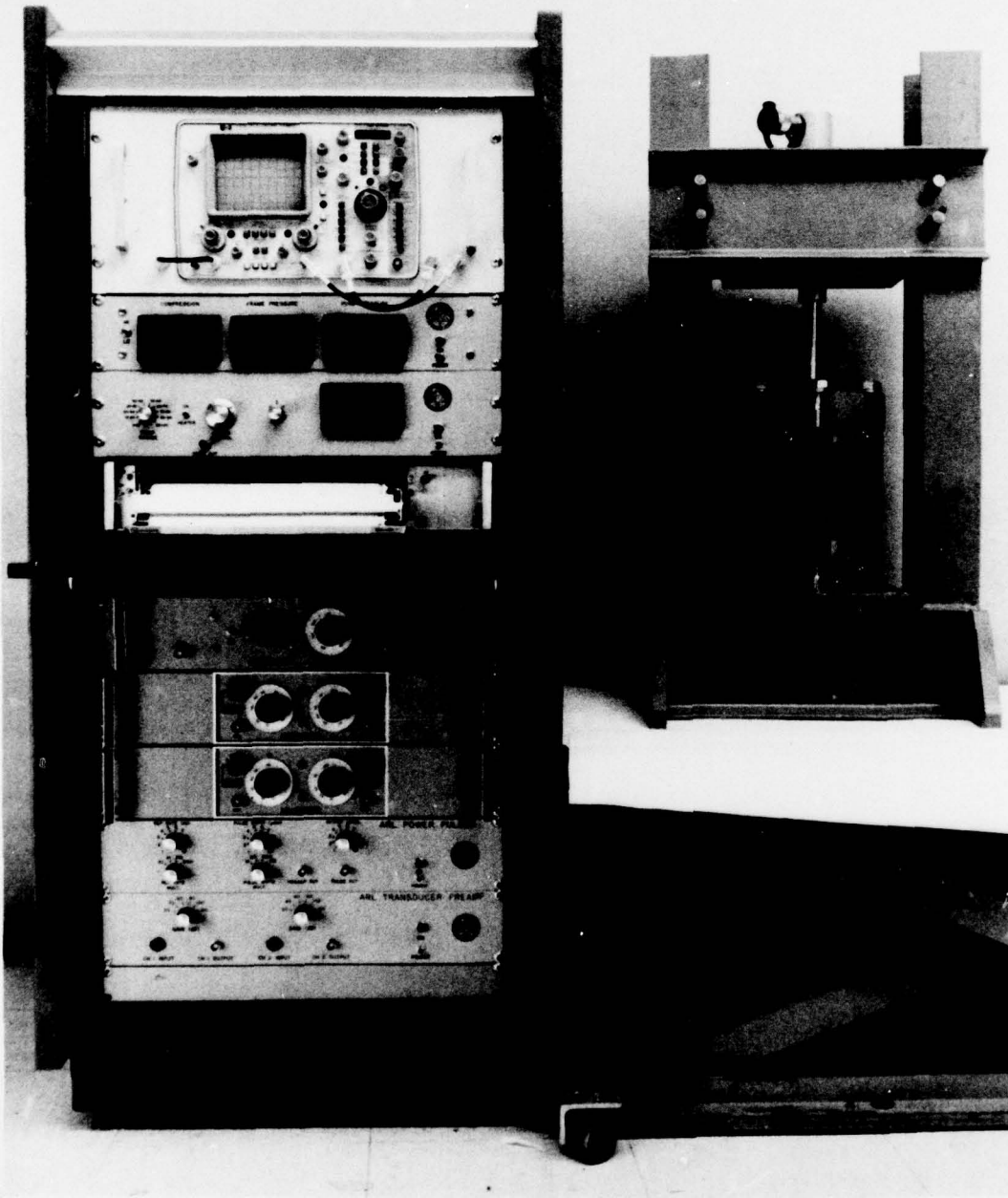


**FIGURE 1**  
**SUBSEAFLOOR ENVIRONMENTAL SIMULATOR SYSTEM**

## II. MECHANICAL SYSTEM

Figures 2 and 3 are photographs of the complete mechanical system of the environmental simulator assembled and disassembled. Various parts of the system are labeled in the figures. Figure 4 is a cross-section line drawing of the pressure chamber.

The stainless steel pressure chamber holds the sediment specimen; it has removable end caps. The top end cap contains a hole with O-ring seals to allow a piston to be moved inside the pressure chamber. The sediment is contained in a stainless steel sleeve (not shown in Fig. 3) which can be placed inside the pressure chamber. The sleeve has thin walls (2.4 mm) and a sharpened edge to allow a sample to be cut from a geophysical core and inserted into the pressure chamber. Dimensions of the sample tube are 55.2 mm i.d. x 156 mm high; the volume of sample contained in the sleeve is thus  $373.3 \text{ cm}^3$ . This quantity is important in calculating volume changes of the sample with overburden pressure applied. The piston is designed to be a close fit inside the sample sleeve; it also has O-ring seals so that none of the sediment can escape past the piston. The face of the piston is covered with a 6.4 mm thick porous stone with drainage holes through the piston behind the stone to allow free movement of the pore fluid into and out of the sediment during tests. Since the motion of the piston during a test must start above the surface of the sediment sample and since the O-rings on the piston would not enter the sample sleeve past the sharp cutting edge without some damage, a guide ring with the same thickness and diameter as the sample sleeve is placed above the sample sleeve and is machined in such a way that the guide ring fits over the cutting edge of the sleeve. Thus the piston starts out inside the guide ring and is smoothly guided into the sample sleeve as the sample is compressed. Total length of guide ring and sample sleeve is the same as the length of the pressure chamber.

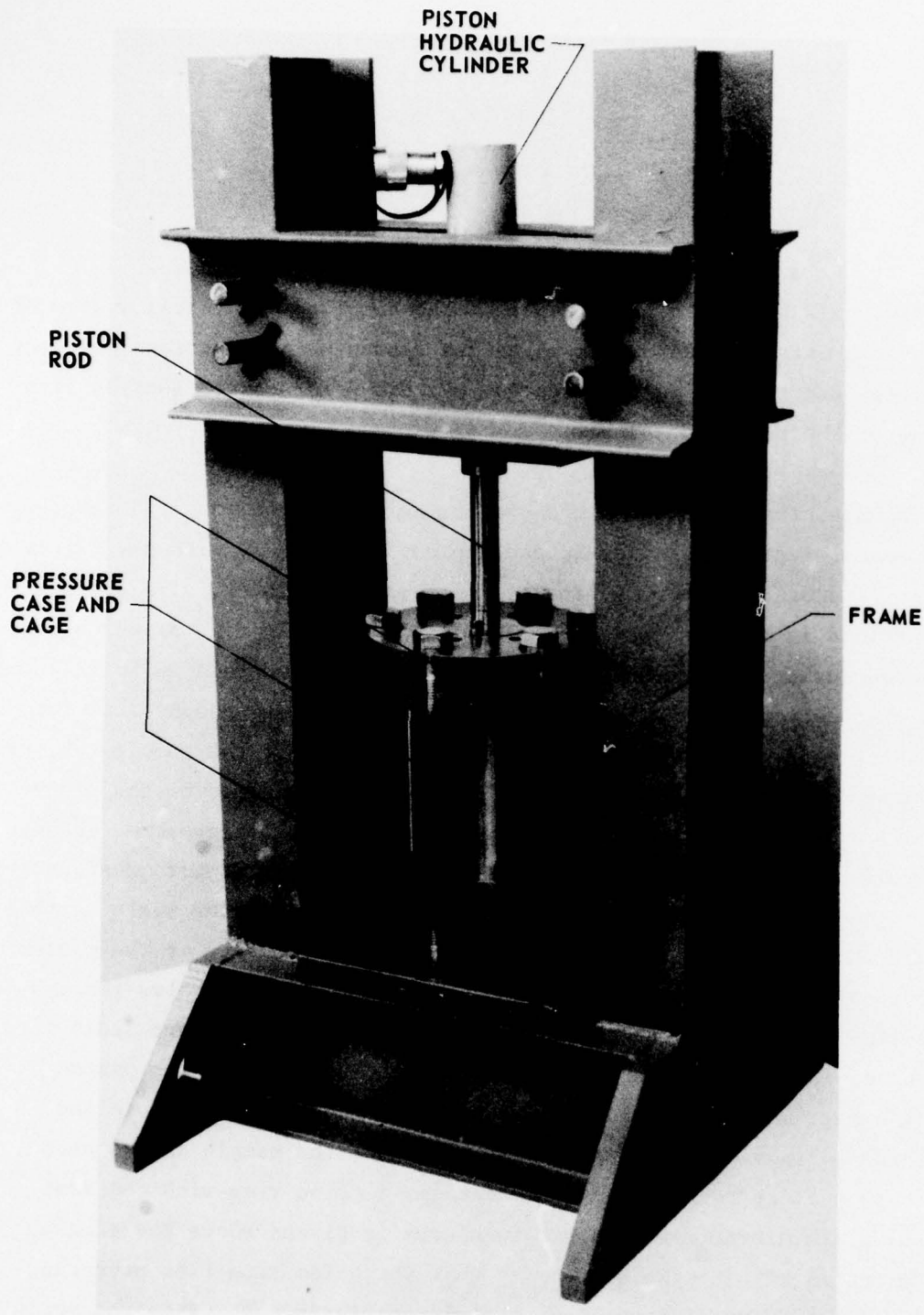


FIGURE 2  
ASSEMBLED PRESSURE CASE AND HYDRAULIC PRESS  
OF THE ENVIRONMENTAL SIMULATOR

3447 - 7

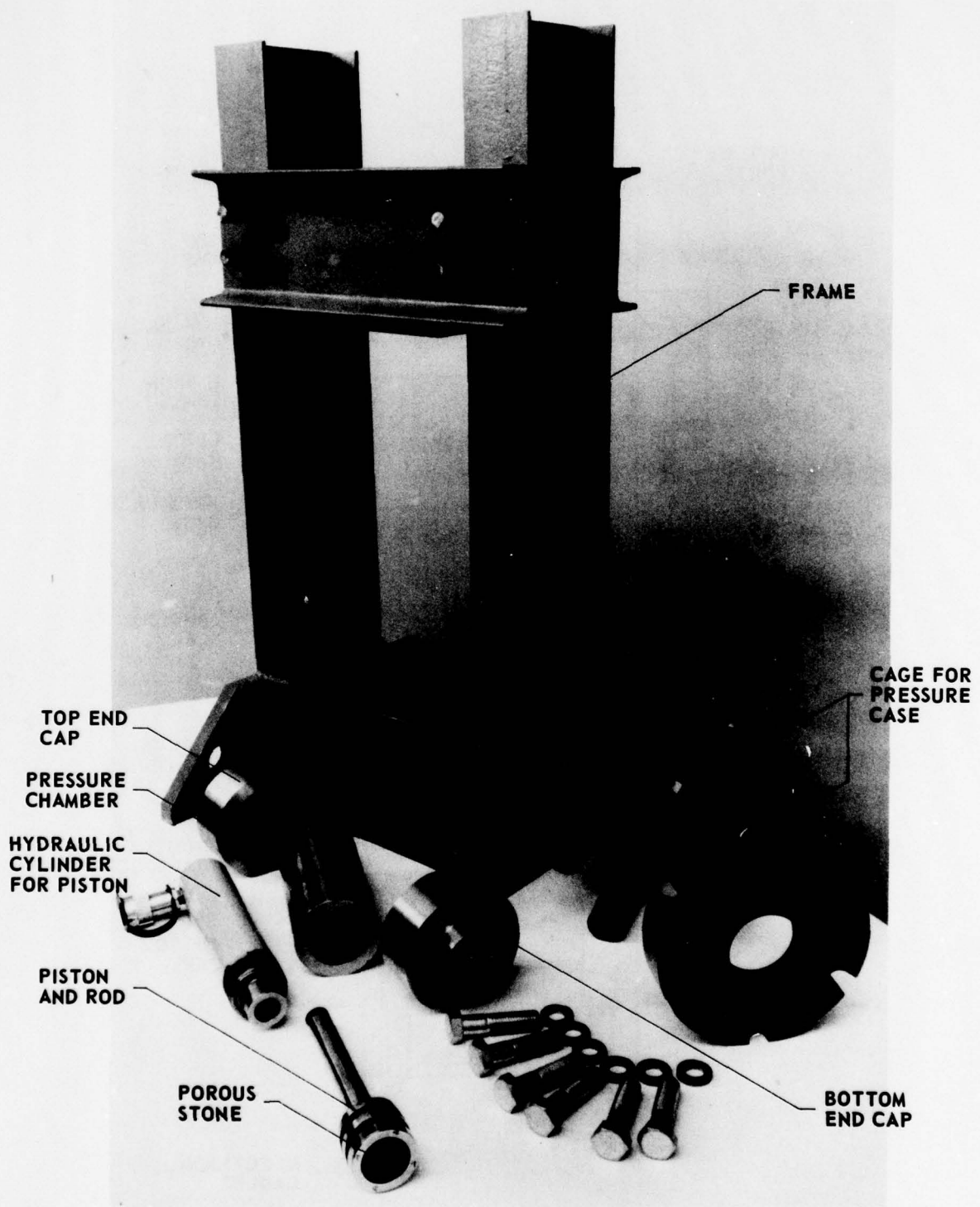


FIGURE 3  
ENVIRONMENTAL SIMULATOR DISASSEMBLED

3447 - 3

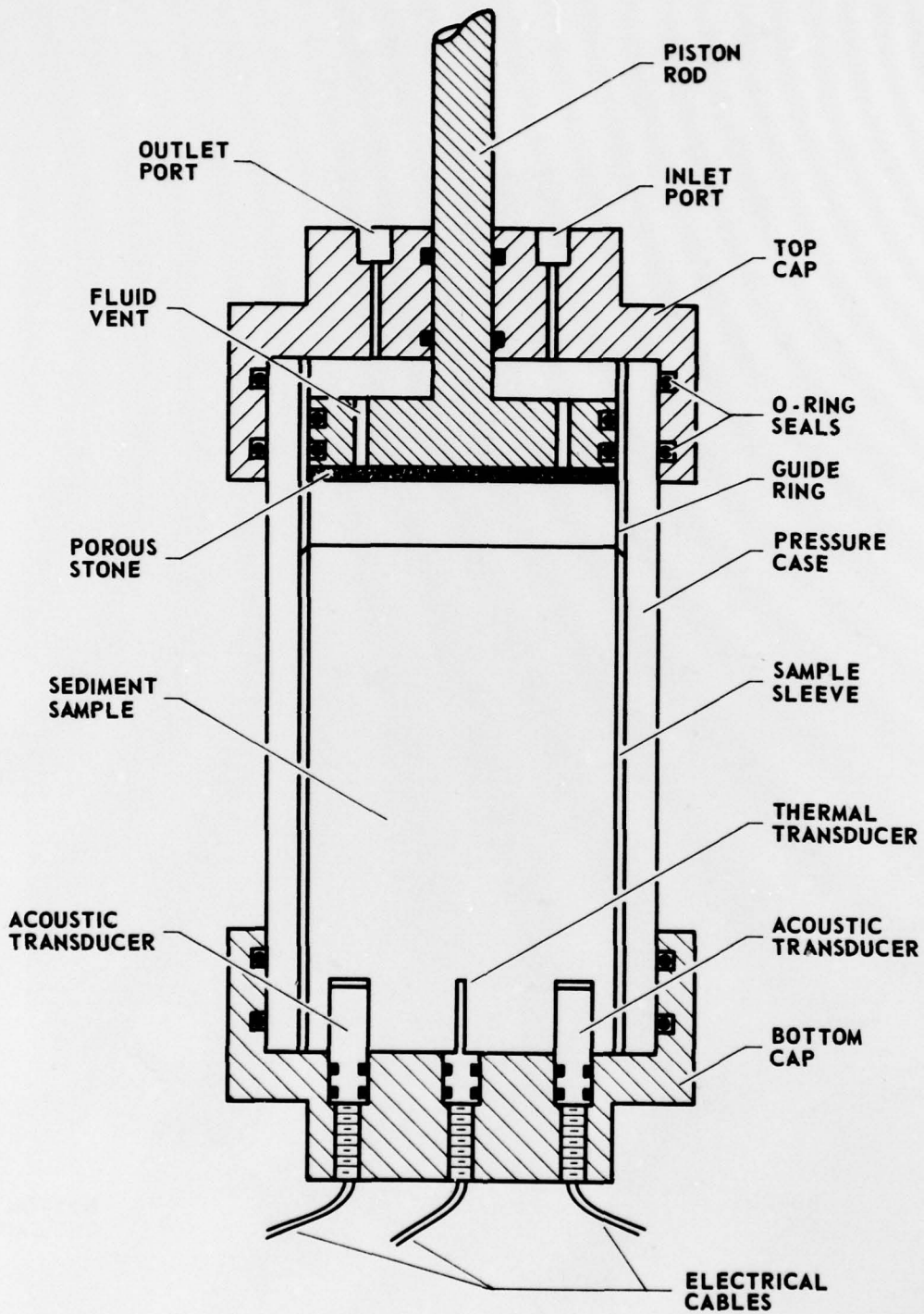


FIGURE 4  
PRESSURE CHAMBER CROSS-SECTION

The bottom end cap of the pressure chamber contains the mounting holes for the acoustic and thermal transducers. Each hole consists of a bottom threaded portion to accept the threaded bases of the transducer mounts and a smooth portion at the top for the O-ring seals on each transducer base. There are three acoustic transducers--one projector and two receivers, and one thermal conductivity transducer. The holes for the three acoustic transducers are arranged such that the two receiver transducers are at different distances from the projector. The thermal probe mounts in the center hole. Blank plugs are supplied so that the system can be used without the transducers.

Figure 5 is a schematic representation of the acoustic transducers designed to be mounted in the environmental simulator chamber. The transducers have both shear wave and compressional wave elements. The shear wave element is a bender 6.35 mm long x 1.59 mm wide and 0.5 mm thick. The bender type element has been used before for generation and detection of shear waves in highly unconsolidated sediments.<sup>1,2</sup> The compressional wave element is a lead zirconate titanate ceramic with dimensions of 3.18 mm x 3.18 mm x 0.79 mm polarized and driven in the thinnest dimension. The elements are mounted on a 25.4 mm x 12.7 mm x 0.79 mm stainless steel blade with appropriate cutouts to receive the transducer elements. The shear wave element is bonded to the metal holder at the back end of the element. The compressional wave element is isolated from the metal holder but held rigidly in place by a polyurethane potting compound which covers the whole area of the blade. The blade is rigidly mounted along its bottom edge to the threaded holder. Small insulated wires are bonded in the plastic coating to connect the active elements to a 4-conductor shielded cable which runs through the bottom of the holder and connects to the electronic system. Projector and receiver transducers are identical and can be interchanged. Utilization of the above design enables the transducers to be easily replaced in case of failure or damage.

The thermal transducer is similar in design to that developed by Von Herzen and Maxwell in 1959.<sup>3</sup> A small thermistor bead is mounted midway inside a 6.35 cm long stainless steel #20 hypodermic needle with a

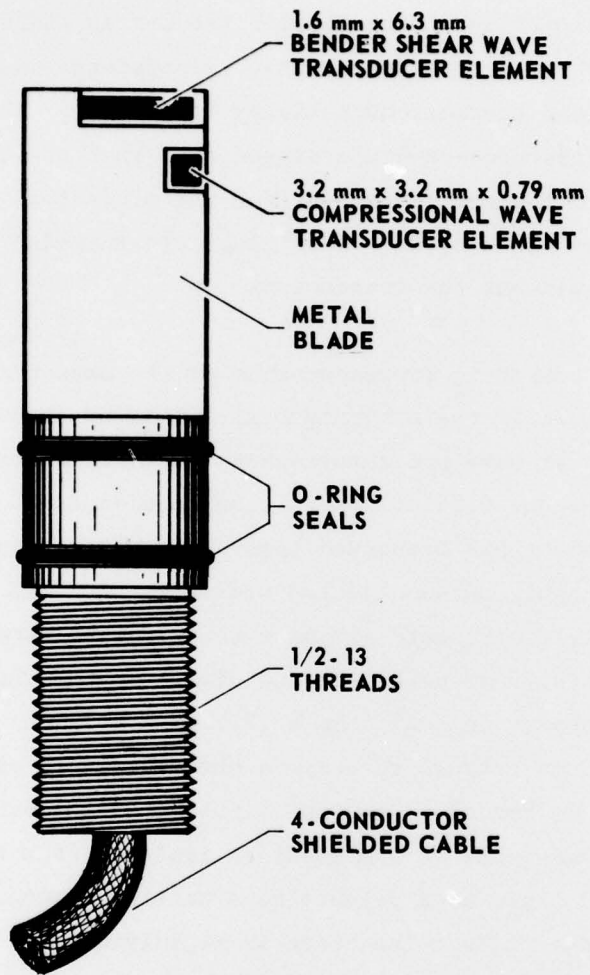


FIGURE 5  
ACOUSTIC TRANSDUCER

fine heater wire loop which runs the length of the needle. The probe is mounted on a base identical to those used for the acoustical transducers. Again, a 4-conductor cable connects the heater wire and thermistor to the electronic measuring system. The thermistor can be used by itself to monitor the temperature of the sample at a point very near the path of acoustical propagation. The heater and thermistor can be used together to measure thermal conductivity of the sample.

Since the pressure inside the chamber would tend to force the end-caps off the chamber, a heavy steel cage is used to hold the pressure chamber together. The cage is shown in Figs. 2 and 3. The pressure chamber-cage combination is designed to be mounted in a heavy steel frame so that a force can be exerted on the piston rod which projects from the top of the pressure chamber. The bottom plate of the frame has appropriate clearance holes for the bolt heads of the cage and also holes through which the electrical cables from the transducers can be placed. The bottom plate is constructed of 19 mm (3/4 in.) thick armor plate steel for maximum strength. The top cross-member of the frame holds the hydraulic cylinder which is used to exert force on the piston. This cross-member is held in place by 4 steel pins and is easily removable so that the pressure chamber and cage can be placed in the frame.

For temperature control of the specimen, a coil of 9.5 mm (3/8 in.) o.d. copper tubing is wrapped around the stainless steel pressure cylinder and is bonded to it by thermally conductive epoxy. This coil is not shown in the figures. To thermally isolate the pressure chamber from the frame when operating far from room temperature, a 6.35 mm (1/4 in.) thick asbestos plate is supplied which has the same dimensions and hole pattern as the bottom plate of the frame.

One of the physical properties of a sediment that is of interest for comparison to the acoustical properties is the porosity of the sediment. To enable calculation of the change in porosity experienced by the sediment in response to changes in overburden pressure, the system incorporates a device to accurately measure the amount of piston displacement. The

measurement device consists of a linear variable differential transformer capable of measuring  $\pm 7.62$  cm ( $\pm 3$  in.) mounted on the frame parallel to the piston hydraulic cylinder. The armature of the transformer is connected by a clamp to the piston rod. A digital display in the equipment rack shows the displacement in two switch selectable ranges. In the low range, the meter will read  $\pm 1.9999$  in. while in the high range the meter will read  $\pm 19.999$  in. in case of large piston displacements. The linear range of the LVDT is  $\pm 7.62$  cm ( $\pm 3$  in.).

The hydraulic system of the simulator consists of two Enerpac hand pumps and two Enerpac 10-ton cylinders. The system is shown in schematic form in Fig. 6. The cylinder that supplies frame pressure to the sample drives the piston and rod directly. The other cylinder is mounted on a small stainless steel cylinder with a piston to supply the pore fluid pressure to the system. Electronic pressure sensors monitor and display hydraulic fluid pressure of the frame pressure system and the pore fluid pressure of the other system over the range of 0-10,000 psi.

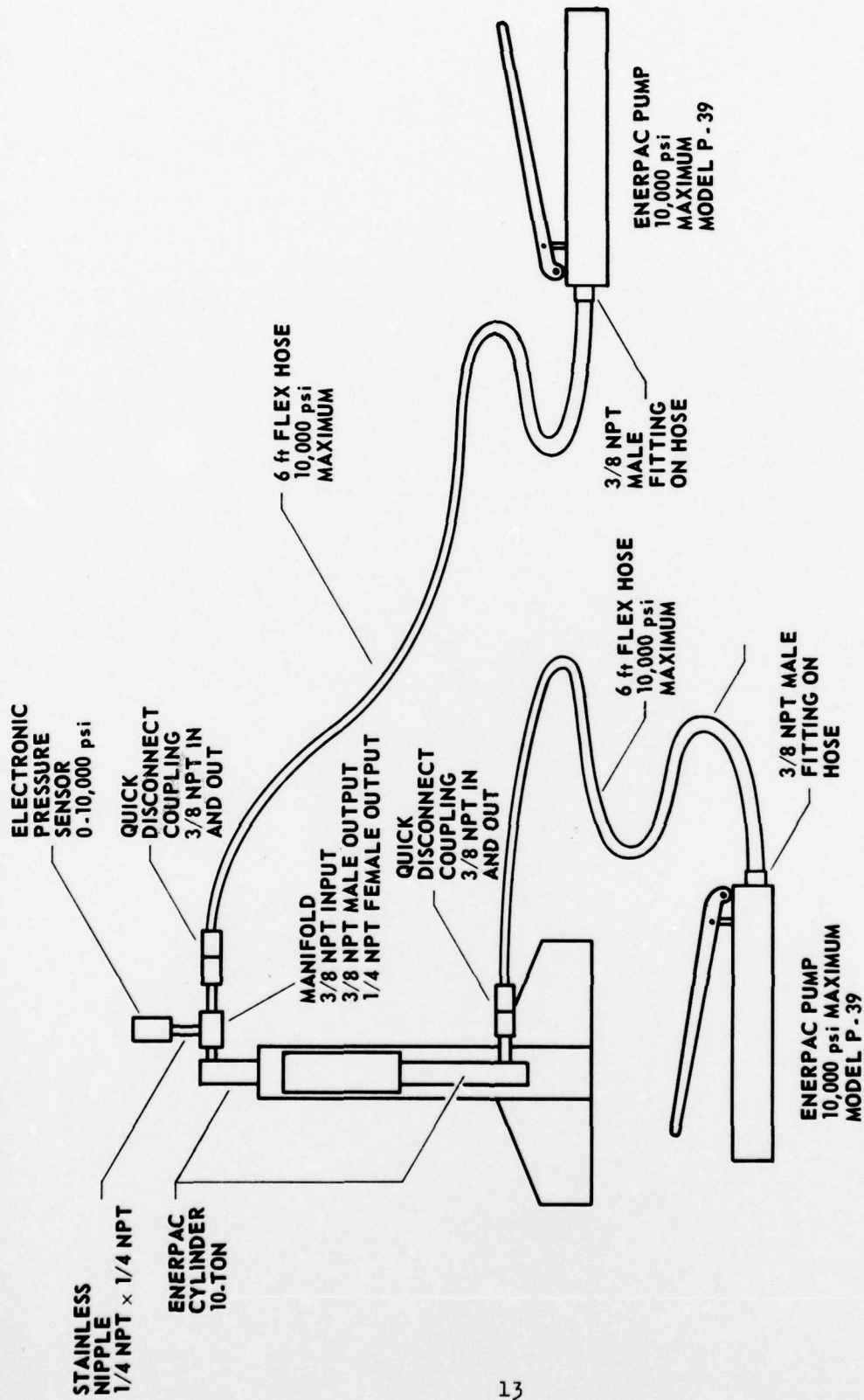


FIGURE 6  
 SUBSEAFLOOR ENVIRONMENTAL SIMULATOR  
 HYDRAULIC SYSTEM

### III. ELECTRONIC SYSTEM

The electronic system of the simulator incorporates all of the measurement electronics in one complete unit; no other equipment is required to make measurements. Figure 7 is a block diagram of the system. There are three subsystems in the unit, one to make acoustical measurements, another to make thermal measurements, and another to measure and display pore pressure, frame pressure, and piston displacement.

#### A. Acoustic Subsystem

The acoustical measurement subsystem consists of a power pulse generator to drive the projector, a dual preamplifier for the receiving transducers, two variable bandpass filters for the received signals, and an oscilloscope to monitor the signals and measure the time difference between the received pulses.

The power pulser drives the projecting transducer with a square pulse of variable amplitude, duration, and repetition rate. The amplitude is variable from 0 to 40 V into a load of 20 to 2000  $\Omega$ . Pulse duration can be varied from 1  $\mu$ sec to 10 msec. Repetition rate can be adjusted from 1 pulse every 10 sec to 1000 pulses/sec. Provision is made to supply a trigger signal to the oscilloscope at the beginning of each transmit pulse.

The preamplifier unit is dual channel and consists of a rack mounted assembly plus small individual units cabled to the rack unit and mounted on the frame of the pressure chamber to be near the receiver transducers. This design allows the high impedance cable between transducer and preamplifier to be short to minimize noise pick-up. The cable connections between the preamplifier boxes and the main unit are low impedance

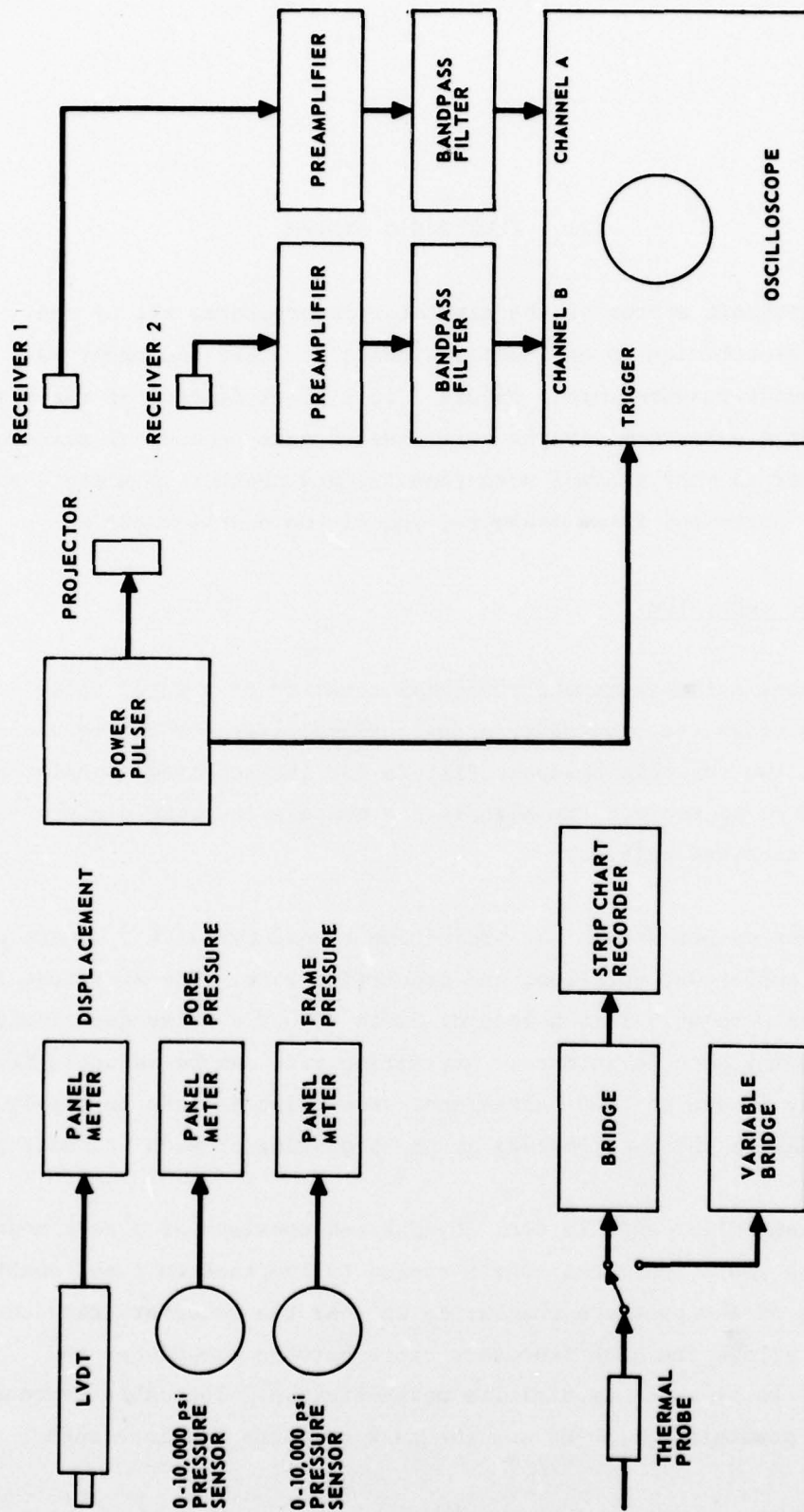


FIGURE 7  
SUBSEAFLOOR ENVIRONMENTAL SIMULATOR  
BLOCK DIAGRAM

allowing long cables with minimum noise pick-up and signal degradation. In this way, the equipment rack and pressure chamber can be separated by several tens of meters without signal degradation from long cable runs.

The power pulser and the preamplifier were both designed and constructed at ARL:UT. A detailed circuit description is presented in Section IV.

The output of each channel of the preamplifier is bandpass filtered by a Krohn-Hite model 3100R solid state variable filter. High and low cutoff frequencies can be independently varied from 10 Hz to 1 MHz. The passband gain is unity (0 dB) and the roll-off is 24 dB per octave outside the passband. The operation and maintenance of the filters is described in detail in the manual supplied with the units.

The amplified and filtered signals are applied to the inputs of a Hewlett-Packard Model 1743A oscilloscope. The oscilloscope is 2-channel with provision for measuring the time difference between two adjustable points on one trace or between one point on one trace and another point on the other trace. The time measurements are accurate to  $\pm 2\%$  at sweep speeds from 50 nsec/div to 20 msec/div and at ambient temperatures of  $+15^{\circ}\text{C}$  to  $+35^{\circ}\text{C}$ . One operating mode of the oscilloscope allows the pulse on one trace to be superimposed on the pulse of the other trace and their time differential ( $\Delta t$ ) measured and displayed digitally. The method of  $\Delta t$  measurement by cycle to cycle matching in overlapped pulses is recognized as the most accurate way of sound speed measurement using pulse techniques.<sup>4</sup>

#### B. Thermal Subsystem

The thermal measuring subsystem consists of the thermal probe, the two measuring bridges and a Leeds and Northrup strip chart recorder. Both of the bridges are laboratory constructed and will be discussed in detail later. One is a variable Wheatstone bridge with calibrated controls in decade resistance ranges with an output for a voltmeter to

indicate when the bridge is balanced. This bridge is for accurate calibration of the thermal probe and measurements when only the temperature of the sample is required. The second bridge is used with the strip chart recorder to measure thermal conductivity. The thermal conductivity bridge includes a digital panel meter which allows measurement of the voltage across and the current through the resistance heater element in the thermal probe. The panel meter also is switch selectable to read temperature. The output of the bridge is recorded as a function of time by the strip chart recorder. Thermal conductivity is measured by recording the change in temperature of the thermal probe imbedded in the sample after a known amount of electrical power is supplied to the heater in the probe.

C. Pressure and Displacement Subsystem

The pressure and displacement subsystem consists of a rack unit to supply power to the two pressure gauges and the differential transformer, each of which has all necessary electronic circuits included in the gauge. The rack unit has three digital panel meters for displaying pressures and displacement. This unit was also constructed at ARL:UT and will be discussed in detail later.

#### IV. ELECTRONIC CIRCUIT DESCRIPTIONS

##### A. Power Pulser

Figure 8 is a schematic of the power pulser unit of the simulator. The circuit incorporates two NE555 integrated circuit timers to provide square pulses at selected repetition rates and pulse widths to a 5-transistor power driver. The driver stage used power field effect transistors to drive the transducer. They were selected because of their lack of secondary breakdown, their thermal stability, and their near indestructibility when properly protected.

IC1 and associated components form an astable multivibrator. The ON time of the output at pin 3 of IC1 is controlled by the sum of R1, R2, and R3 and the capacitance selected by the REPETITION RATE MULTIPLIER control S1. The OFF time of the output is controlled by R3 and the selected capacitor. By properly setting S1 and R1 the ON time can be varied from 1 msec to 10 sec thus giving a repetition rate from 1000 pps to 0.1 pps. The output at pin 3 of IC1 is coupled to the monostable multivibrator circuit formed by IC2 and associated components. C7 and R4 form a differentiating network to shorten the pulse applied to the trigger input, pin 2 of IC2. Each time pin 2 of IC2 is pulled toward ground by the pulse from IC1, the output of IC2, pin 3, goes to +5 V and remains there for a time interval determined by R5, R6, and the capacitor selected by the PULSE WIDTH MULTIPLIER control S2. By properly setting R5 and S2 the pulse width can be varied from 1  $\mu$ sec to 10 msec. The pulse at the output of IC2 is supplied to the TRIGGER OUT connectors on the front and rear panels of the unit and also drives the power driver circuits. Q1 inverts the pulse from IC2. The inverted pulse drives Q2, which inverts the pulse again and transforms the +5 V level up to +36 V level. The high level pulse drives emitter follower Q3 which has the

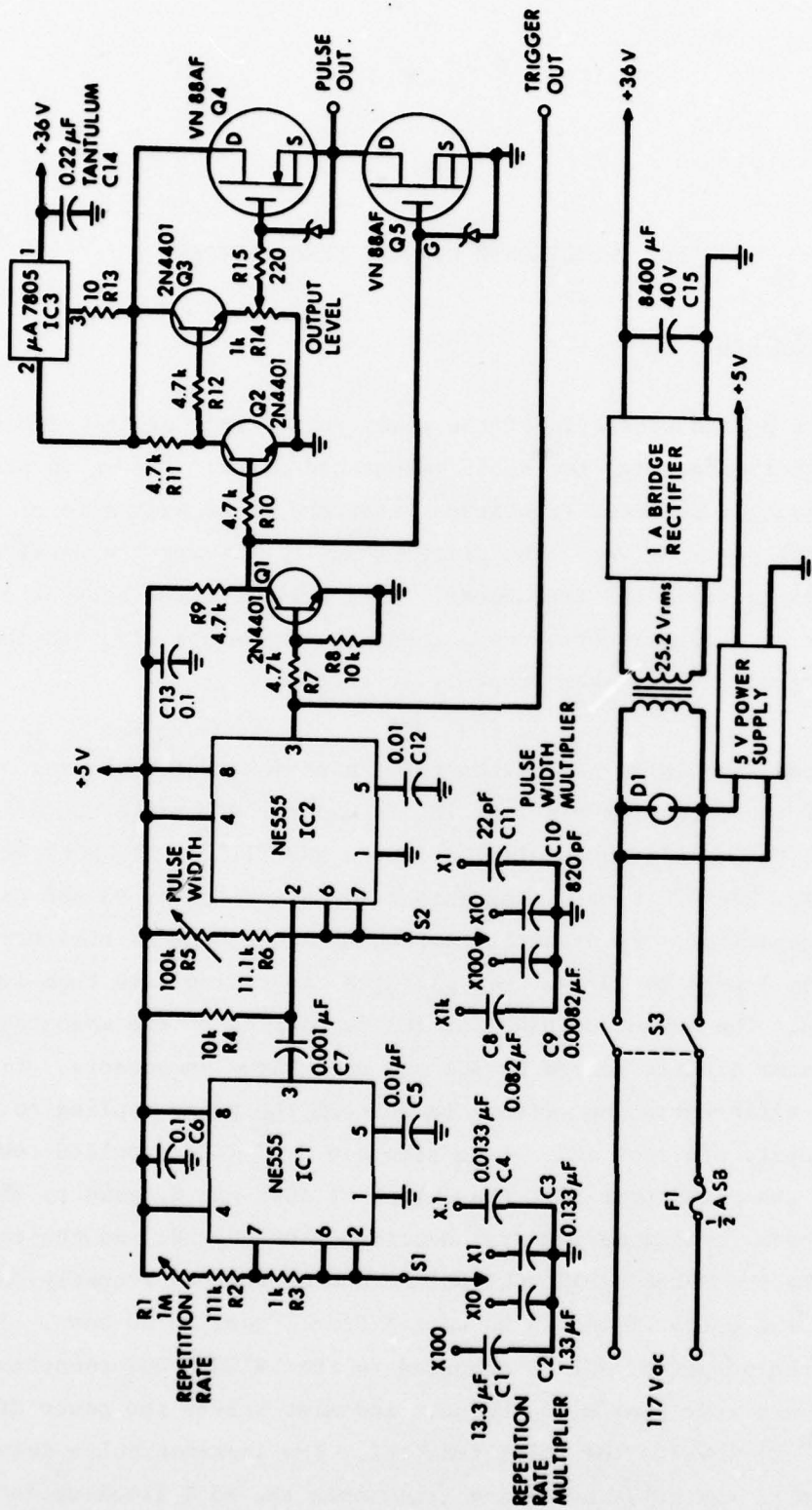


FIGURE 8  
POWER PULSER SCHEMATIC DIAGRAM

ARL:UT  
AS-79-2172  
DJS - GA  
11-8-79

OUTPUT LEVEL control R14 as emitter resistor. A variable level pulse is tapped off by the slider of R14 to drive Q4, which is a power FET wired as a source follower to drive the load applied to the PULSE OUT connector on the front panel. Q5 is driven 180° out of phase with Q4 and acts to clamp the output line to ground during the periods between pulses. Clamping the output reduces ringing of the transducer and shortens the acoustic pulse that is generated. IC3 and R13 form a current limiter for the output stage. The power FET is capable of carrying 2 A of current. However, the current supply to the final stage is limited to 0.5 A so that the output transistor is protected if the output is shorted to ground.

#### B. Preamplifier

Figure 9 is a schematic of one channel of the preamplifier. Both channels are identical and the unit incorporates a single power supply for both channels.

Each preamplifier circuit is in two sections, one housed in a small aluminum box to be placed near the transducer, the other, in the rack panel. Four-conductor shielded cable connects the transducers to the preamplifier box through P1 and SC1, and also connects each box to the rack unit.

IC4 and IC5 form a differential input/differential output amplifier with 20 dB gain; R19, R20, and R21 set the gain. R16 limits the input impedance to 10 MΩ. S4 selects either the shear wave or compressional wave transducer, shorting the unused transducer to ground to eliminate feedover interference.

IC6 forms a variable gain differential input/single output stage. IC7 is a single input/single output stage with variable gain. The gain-setting resistors selected by switch S5 vary the gain of the final two stages from 0 to 100 dB in 20 dB steps. Since the first stage has a constant gain of 20 dB, the total gain of the complete circuit can be

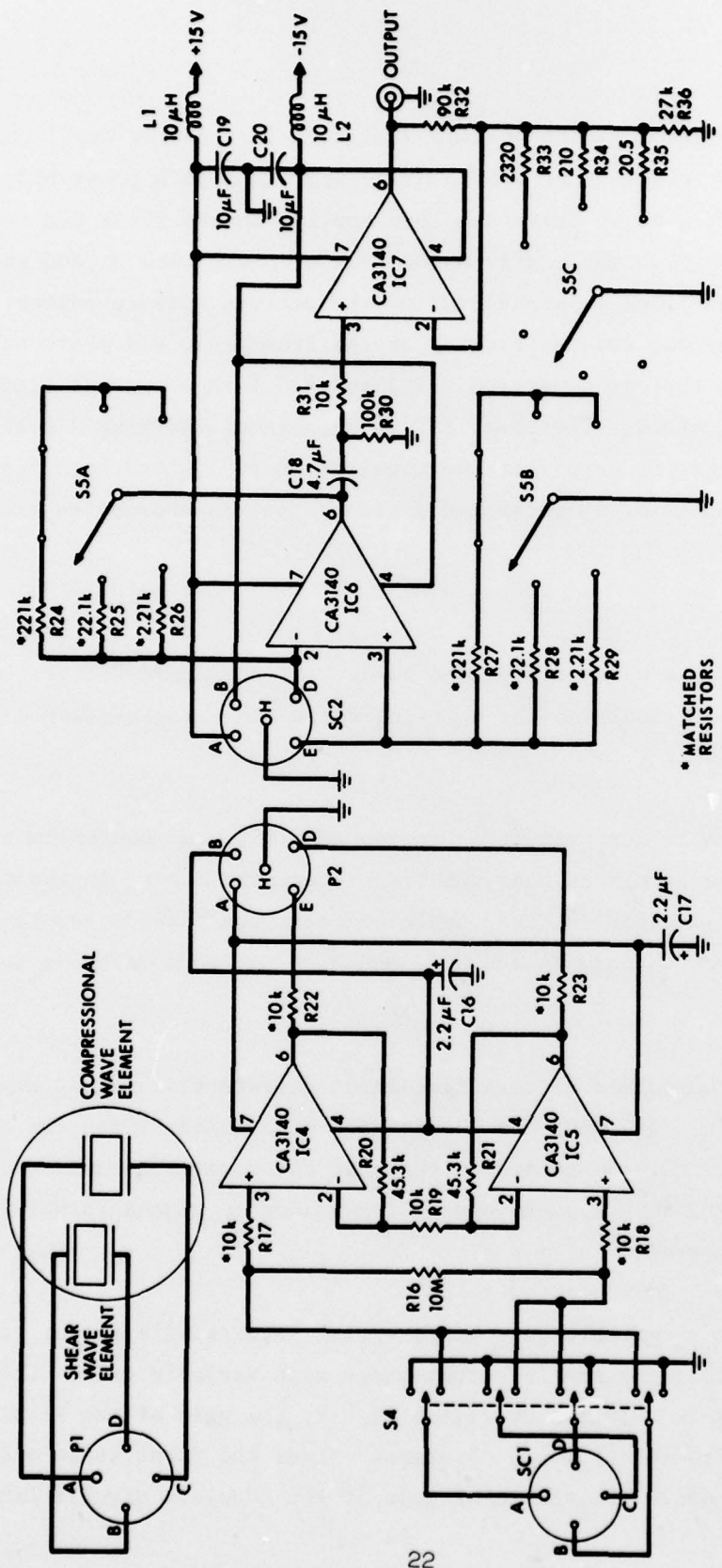


FIGURE 9  
PREAMPLIFIER SCHEMATIC DIAGRAM

varied from 20 dB to 120 dB. C18 and R30 form an ac coupling circuit so that dc offset at high gain settings does not saturate the final stages.

#### C. Thermistor Bridge

Figure 10 is a schematic of the thermistor bridge. The circuit is a standard Wheatstone bridge with 4 decade resistor switches. A socket on the front panel accepts the plug on the cable from the thermal conductivity probe. Switch S6 connects the battery supply to the circuit. The bridge is connected to two phone tip jacks on the front panel. The output can be monitored at these jacks by a voltmeter to detect the point at which the bridge is balanced by the switchable decade resistors; the bridge is balanced when the output is zero. The thermistor resistance is then read off the decade switch knobs on the front panel of the unit.

#### D. Thermal Conductivity Bridge

The thermal conductivity measuring unit is used with the thermal conductivity probe which is mounted in the pressure case to measure the thermal conductivity of a sediment sample at various pressures and temperatures. Figure 11 shows a block diagram of the electronic unit. SC3 is the input socket on the rear panel of the unit for the thermal probe plug. Pins A and B on the plug connect to the heater in the probe; pins C and D connect to the thermistor. Switch S7 selects the data displayed on the digital panel meter. In the E position the meter displays the voltage across the probe heater element and in the I position displays the current through the heater. In the T position the meter displays the temperature that is measured by the probe thermistor and thermistor bridge. The panel meter has an input range of 0 to 1.999 V. R43, R44, R45, and R46 form a divide-by-ten network to reduce the heater voltage (0-12 V) to the range of the meter. Current through the heater is measured by detecting the voltage across R47, which is a 10  $\Omega$  resistor in series with the heater. The differential amplifier following S7A and S7B is an X1 gain amplifier required to remove the voltage offset due to R47 from the heater voltage reading. S7D selects the proper

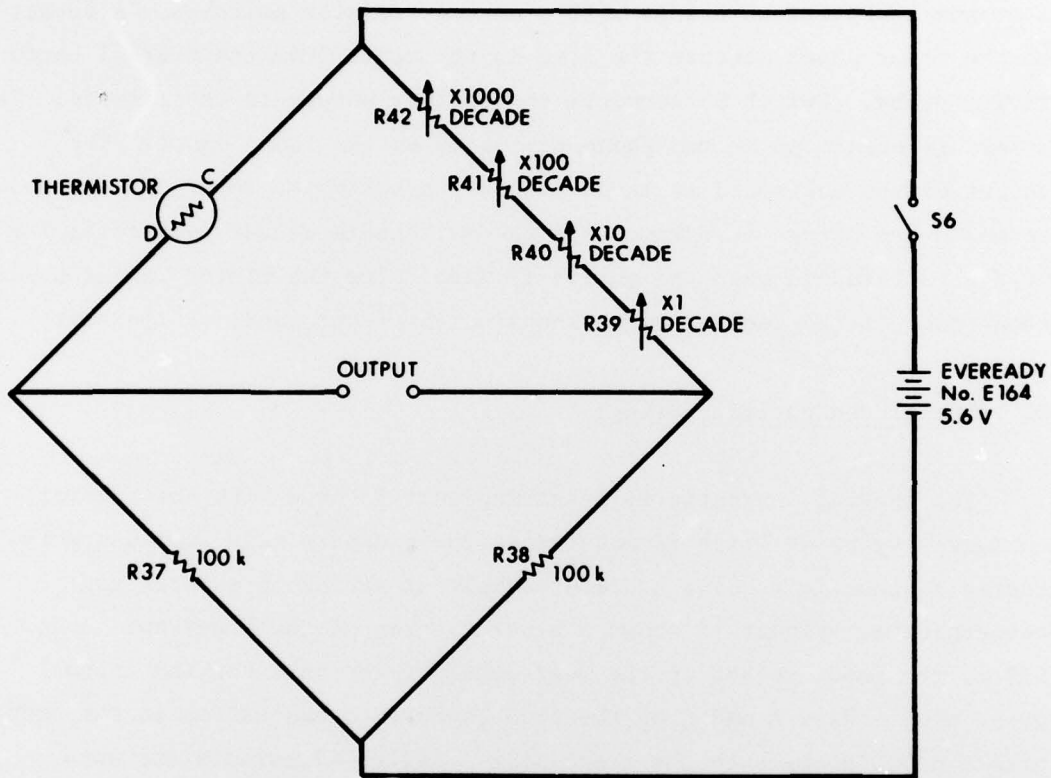


FIGURE 10  
THERMISTOR BRIDGE SCHEMATIC DIAGRAM

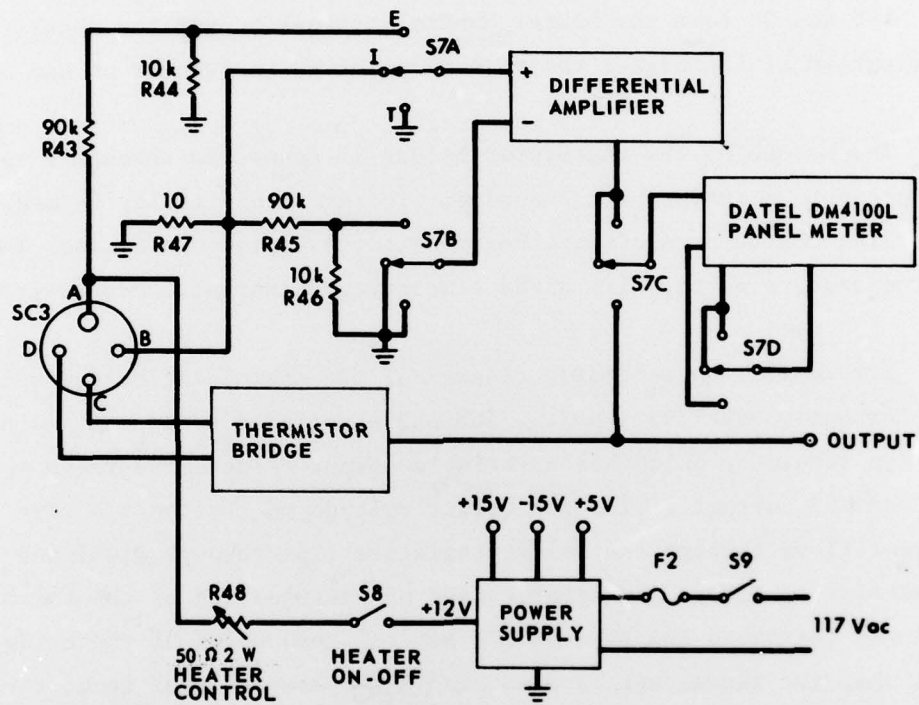


FIGURE 11  
THERMAL CONDUCTIVITY BRIDGE BLOCK DIAGRAM

position of the decimal point on the meter display. In the temperature mode the meter displays a range of 19.999°C while a range switch in the thermistor bridge circuit selects 10°C ranges from 0° to 100°C. Thus the actual temperature is the sum of the range switch reading and the meter reading. For example, if the range switch is set to 10° and the meter reads 5.000, then the temperature is 15.000°C.

R48 and S8 form the heater control circuit to set the power dissipation of the heater and to turn power to the heater on and off.

The output of the thermistor bridge is connected through a rear panel connector to a strip chart recorder. Thermal conductivity is measured by recording the temperature of the probe for a period of 10 min. The slope of temperature versus time gives a measure of thermal conductivity.<sup>3</sup>

Figure 12 is a schematic diagram of the thermistor bridge section of the thermal conductivity unit. IC8 and associated components form a low voltage regulator which has a variable output selected by range switch S10. R52 and R53 further divide the output voltage so that only a very small current flows through the bridge resistors (R64 through R103) and the thermistor to reduce the error caused by self-heating of the thermistor. Variable resistors R64 through R73 set the zero point of the bridge so that when the thermistor is measuring a temperature that is at the midpoint of a temperature range, the output of IC9 can be set at 0 V. Calibration resistors R54 through R63 control the span of the bridge so that when the thermistor is measuring a temperature at the bottom end of a range, the output of IC9 can be set to -5.000 V. Each range of the bridge has a set of calibration controls. IC10 provides a variable offset to the output of IC9 so that when measuring a temperature at the bottom of a range, the output from IC10 is 0 V and at the top end it is +10.000 V. The offset is controlled by R114.

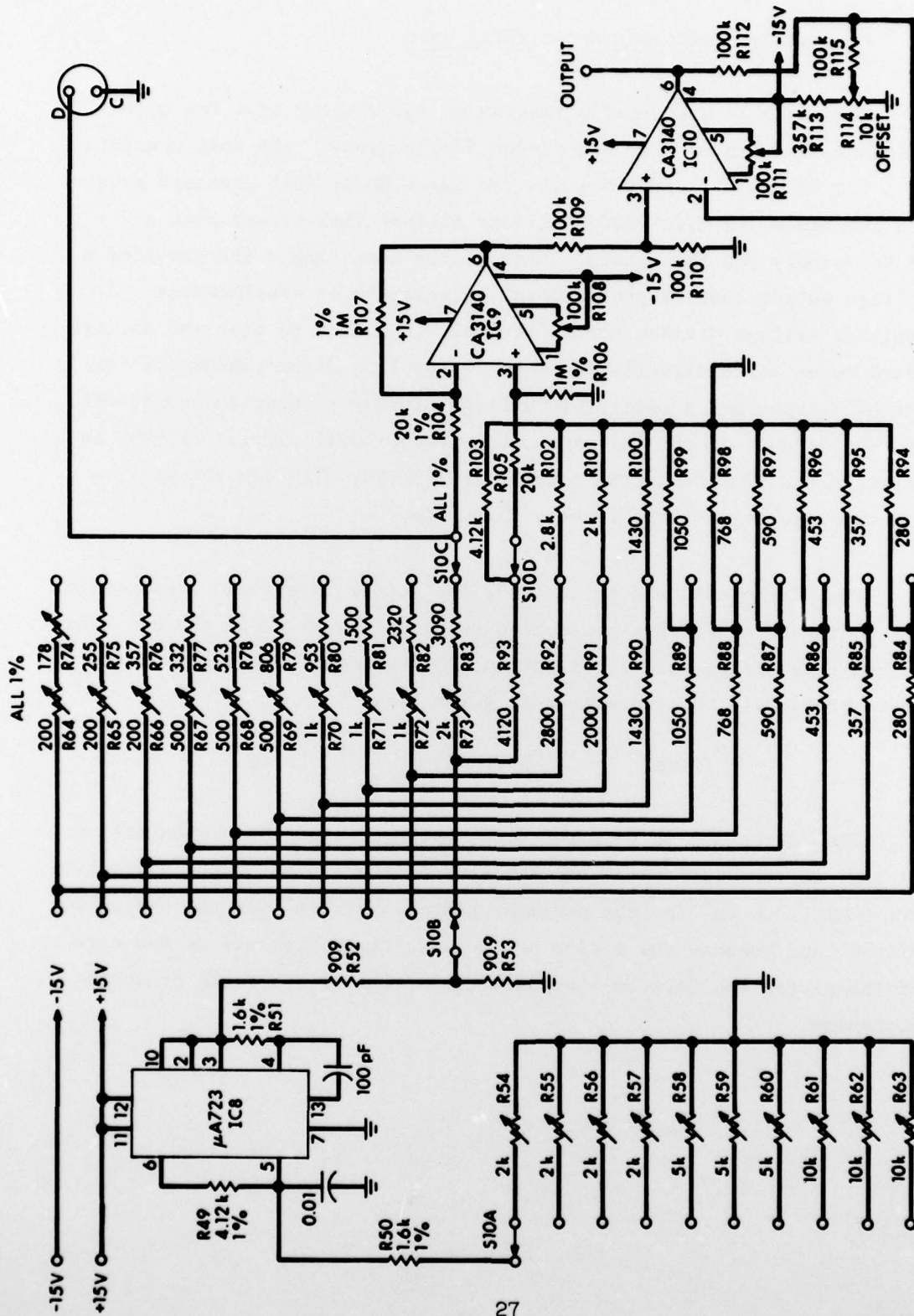


FIGURE 12  
THERMISTOR BRIDGE SCHEMATIC DIAGRAM

ARL:UT  
AS-79-2176  
DJS-GA  
11-8-79

#### E. Pressure and Displacement Display Unit

Figure 13 is a schematic diagram of the display unit for pore pressure, frame pressure, and piston displacement. The unit consists of a +24 Vdc power supply for the two Setra Model 204E pressure gauges and the Schaevitz Model 3000HR linear differential transformer and a +5 Vdc supply for the meters. Each of the measuring units provides a voltage output that is proportional to pressure or displacement. A resistor voltage divider scales the voltage output so that the digital panel meter reads directly in pressure (psi) or displacement (inches). The LVDT input has a switchable voltage divider to provide two levels of resolution. In the low range, the readout will display  $\pm 1.9999$  in., while in the high range the display is  $\pm 19.999$ , although the maximum linear range of the LVDT is only  $\pm 3.000$  in.

The pore pressure display reads the actual pore fluid pressure in the sediment. The frame pressure display, however, reads the hydraulic system pressure so that a correction must be made to obtain the actual frame pressure. The correction is given by:

$$P_{\text{frame}} = 0.610 P_{\text{hydraulic}} - 0.188 P_{\text{pore}} \quad (1)$$

The correction is required because the area of the piston acting on the sediment is larger than the area of the piston in the hydraulic cylinder ( $23.6 \text{ cm}^2$  for the sediment piston,  $14.4 \text{ cm}^2$  for the hydraulic piston) and because the action of the pore fluid pressure on the area of the piston rod ( $4.4 \text{ cm}^2$ ) opposes the action of the frame pressure mechanism.

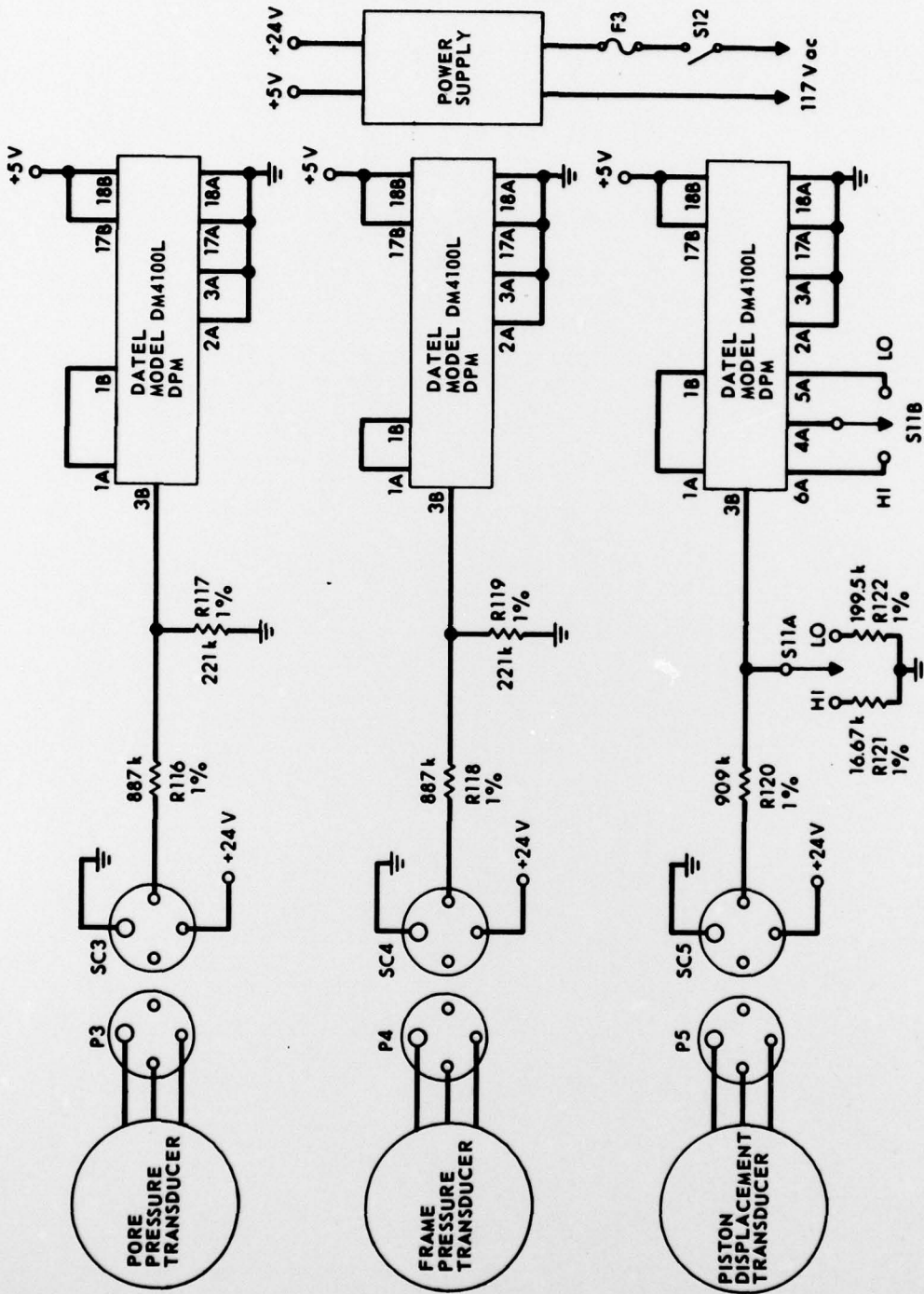


FIGURE 13  
PRESSURE AND DISPLACEMENT DISPLAY UNIT  
SCHEMATIC DIAGRAM

## V. CALIBRATION

Calibration procedures for the commercial electronic units in the simulator system are described in detail in the technical manuals supplied with the equipments. The only calibrations that can easily be carried out on the rest of the system are the determination of acoustic transducer spacing and sensitivity and the calibration of the thermal conductivity measuring unit.

Determination of transducer spacing is done with distilled water in the sample chamber. Since the compressional wave speed of sound in distilled water over a large temperature range is accurately known and listed in a number of handbooks, the separation between the two receivers can be calculated by measuring the time differential between the two received pulses and the temperature of the water in the chamber. The separation,  $D$ , is calculated as follows:

$$D = \Delta t c \quad , \quad (2)$$

where  $c$  is the speed of sound in water at the measured temperature and  $\Delta t$  is the difference in time between reception of the pulses at the two receivers. Since the shear wave and compressional wave elements are rigidly bonded together in the transducer, the same spacing determined for the compressional wave elements can be assumed for the shear wave elements.

Sensitivity of the compressional wave elements can be determined with relative ease because distilled water has such a low attenuation factor that it can be assumed to be zero. Thus the difference in amplitude between the received pulses from the compressional wave elements is due to spreading loss and differences in sensitivity, both of which should remain constant as long as the transducers are not disturbed. Thus, any

changes in amplitude of the received signals can be interpreted as attenuation when another medium replaces the water. The measurements are complicated, however, by the fact that the sensitivity of each element is a function of ambient temperature and does not necessarily track the response of the other element. So, if attenuation measurements are to be made as a function of temperature, the water calibration must be made over the same temperature range.

Due to the lack of a medium for shear wave propagation with consistent properties and that can readily be placed in the test chamber, an accurate attenuation calibration of the shear wave transducers cannot easily be made. However, a dry sand such as Ottawa sand will generally come to the same state of compaction each time it is placed in the container if it is allowed to fall, a small amount at a time, from a height of at least 1 m. The shear wave speed and attenuation for such a sample is thus repeatable to a degree. A rough calibration of the shear wave transducers can then be made by measuring the received pulse amplitudes with the receiver transducers in one configuration and then with their positions switched. The difference in amplitudes of the signals from each transducer when in the near and far positions should match that of the other transducer and is the signal loss due to spreading and attenuation. Thus the actual sensitivity of each transducer can be calculated.

For calibration of the thermistor in the thermal conductivity probe, an accurate temperature measuring device such as a quartz thermometer or platinum resistance thermometer is necessary. The temperature measuring device and the probe can be placed together in the Lauda circulating bath so that temperature can be varied. With the probe connected to the variable bridge unit, the resistance of the thermistor is determined at closely spaced intervals over the temperature range 0°C to 75°C. The data are plotted and a curve of resistance versus temperature determined for the thermistor. Once the resistance curve has been found, the thermal conductivity unit can be calibrated. A decade resistance box is connected to pins C and D of the input plug of the thermal conductivity unit. The

range switch on the unit is set to the 0° to 10°C range and the display mode switch is set to T. The decade resistor box is set to the equivalent resistance of the thermistor at 5°C. Referring to Fig. 12, the output of IC9 (pin 6) and the wiper of R114 are grounded while R111 is varied so that the panel meter reads 0.000 V. The ground is removed from the wiper of R114 and this resistor is adjusted so that the meter reads 5.000 V. Next the wipers of switches S10C and S10D are grounded. R108 is adjusted to bring the meter reading back to 5.000. The grounds are then removed from the switch wipers. R73 is then adjusted so that the meter reads 5.000. The decade resistance box is changed to the resistance for 0°C and R54 adjusted so that the meter reads 0.000 V. The resistance box is returned to the 5° setting and R73 readjusted if necessary. Repeat the procedure until no further adjustment is necessary to the two controls. Set the range switch to the 10° to 20° range and set the decade resistor to a resistance equal to the 15°C value for the thermistor. Set R72 for a meter reading of 5.000 V. Set the decade resistance to the 10°C value and adjust R55 for 0.000 V on the meter. Repeat these steps for all the temperature ranges of the unit, first setting the decade resistance box to a resistance equivalent to the center of the range, and then to the bottom of the range. After the initial adjustment, R108, R111, and R114 need not be readjusted.

#### ACKNOWLEDGMENTS

This work was supported under contract by NORDA, Code 360. Design and construction of the pressure vessel system was done under the supervision of Dale W. Evertson at ARL:UT.

#### REFERENCES

1. D. J. Shirley, "An Improved Shear Wave Transducer", J. Acoust. Soc. Am. 63, 1643-1645 (1978).
2. D. J. Shirley and L. D. Hampton, "Shear Wave Measurements in Laboratory Sediments", J. Acoust. Soc. Am. 63, 607-613 (1978).
3. R. Von Herzen and A. E. Maxwell, "The Measurement of Thermal Conductivity of Deep Sea Sediments by a Needle-Probe Method", J. Geophys. Res. 64, 1557-1563 (1959).
4. E. P. Papadakis, "Ultrasonic Phase Velocity by the Pulse-Echo-Overlap Method Incorporating Diffraction Phase Corrections", J. Acoust. Soc. Am. 42, 1045-1051 (1967).

29 November 1979

DISTRIBUTION LIST FOR  
ARL-TR-79-53  
FINAL REPORT UNDER CONTRACT N00014-77-C-0779

Copy No.

	Commanding Officer Naval Ocean Research and Development Activity NSTL Station, MS 39529
1	Attn: R. R. Goodman (Code 110)
2	S. Marshall (Code 340)
3	J. Matthews (Code 362)
	Commanding Officer Office of Naval Research Arlington, VA 22217
4	Attn: T. Pyle (Code 48B)
5	M. Odegard (Code 48D)
6	Code 1021P
7	Office of Naval Research Branch Office Chicago 536 South Clark Street Chicago, IL 60605
8 - 13	Director Naval Research Laboratory Department of the Navy Washington, DC 20375
14 - 25	Commanding Officer and Director Defense Documentation Center Defense Services Administration Cameron Station, Building 5 5010 Duke Street Alexandria, VA 22314
26	Office of Naval Research Resident Representative Room No. 582 Federal Building Austin, TX 78701
27	Environmental Sciences Division, ARL:UT
28	Glen E. Ellis, ARL:UT

Distribution List for ARL-TR-79-53 under Contract N00014-77-C-0779

Copy No.

29	Dale W. Evertson, ARL:UT
30	Loyd D. Hampton, ARL:UT
31	Reuben H. Wallace, ARL:UT
32	Library, ARL:UT
33 - 41	Reserve, ARL:UT